Value of Fluorine-18-Fluorodeoxyglucose and Thallium-201 in the Detection of Pancreatic Cancer

Tetsuro Inokuma, Nagara Tamaki, Tatsuo Torizuka, Tohru Fujita, Yasuhiro Magata, Yoshiharu Yonekura, Gakuji Ohshio, Masayuki Imamura and Junji Konishi

Departments of Nuclear Medicine and Brain Pathophysiology; First Department of Surgery, Kyoto University Faculty of Medicine, Kyoto, Japan

This study compares the diagnostic value of ^{18}F-FDG PET imaging and ^{201}Tl-SPECT imaging in patients with pancreatic cancer. **Methods:** Twenty-five patients with histologically-proven pancreatic cancer were studied. Following PET transmission scanning, 3 mCi of ^{201}Tl were administered after patients had fasted overnight. Thallium-201-SPECT images were obtained 15 min later. Immediately after ^{201}Tl-SPECT imaging, 4 mCi of FDG were administered and PET images were obtained 60 min later. The PET and SPECT images were compared qualitatively and quantitatively. For quantitative analysis, 10 × 10 mm^2 regions of interest (ROIs) were selected in areas of the tumor showing the highest tracer accumulation and in the normal pancreas. The tumor to nontumor activity ratio (T/N ratio) was calculated. **Results:** Although both techniques delineated focal lesions with an increase in tracer accumulation in 16 patients, PET identified eight additional patients in whom ^{201}Tl-SPECT images did not visualize any lesion. Thus, FDG-PET provided significantly higher sensitivity (96%) than ^{201}Tl-SPECT (64%). Among the patients showing increased tracer accumulation, the T/N ratio was significantly higher with FDG-PET (3.24 ± 1.27) than with ^{201}Tl-SPECT (1.77 ± 0.37) ($p < 0.0001$). **Conclusion:** We conclude that FDG-PET has a larger clinical value for noninvasive detection of pancreatic cancer than ^{201}Tl-SPECT. If a PET camera is available, FDG-PET is considered to be the method of choice for the evaluation of patients with suspected pancreatic cancer.

Key Words: PET; pancreatic cancer; thallium-201; fluorine-18-fluorodeoxyglucose

J Nucl Med 1995; 36:229–235

Pancreatic cancer is one of the most malignant neoplasms, with an usually poor prognosis (*1*). Accurate diagnosis is of clinical importance for appropriate treatment.

PET imaging with FDG has a potential value for delineating viable tumor tissue on the basis of increased glucose metabolism in the tumor. Experimental (*2–7*) and human (*8–15*) studies have demonstrated an increase in FDG uptake in malignant tumors. A recent preliminary report indicated the value of FDG-PET in the diagnosis of human pancreatic cancer (*16*). However, the need for an expensive PET camera and a cyclotron may limit the clinical application of this technique to patients with suspected pancreatic cancer.

Thallium-201 has also been used for the clinical diagnosis of malignant tumors (*17–20*). Accumulation of ^{201}Tl was observed in viable tumor tissue (*21,22*), reflecting the proliferative potential of tumor cells on the basis of Na-K-ATPase activity (*23*). Togawa et al. (*24*) recently reported the value of ^{201}Tl-SPECT for detection of pancreatic cancer.

MATERIALS AND METHODS

Patients

Twenty-five patients (15 males, 10 females) with histologically-proven pancreatic cancer participated in this study. Patients age ranged from 37 to 77 yr, with a mean of 59 yr. All tumors were histologically confirmed by surgical operation 5 to 26 days after the radionuclide study. They consisted of 20 pancreatic adenocarcinomas, four mucinous cystadenocarcinomas and one ampullary carcinoma. None of the cases had insulin-dependent diabetes, and all patients were in a euglycemic condition during the study. Each patient gave written informed consent as required by Kyoto University's Human Study Committee.

Preparation of Fluorine-18-FDG

Fluorine-18 was produced by ^{20}Ne(d, α)^{18}F nuclear reaction, and ^{18}F-FDG was synthesized by the acetyl hydrofluorite method (*25,26*).

Thallium-SPECT

After overnight fasting and with the subject at rest, 111 MBq (3 mCi) of ^{201}Tl-chloride was injected into a peripheral vein, and ^{201}Tl imaging was begun 15 min later. SPECT was performed using a single-head rotating gamma camera system (General Electric; STARCAM 3000) equipped with a general-purpose collimator, collecting 64 projection images for 20 sec each over 360°. Total acquisition time was approximately 25 min. The slice thickness was 5.8 mm. A series of transverse slices were reconstructed with filtered back-projection using a Ramp Hanning filter with a

Received Feb. 2, 1994; revision accepted June 23, 1994.

For correspondence or reprints contact: Tetsuro Inokuma, MD, Department of Nuclear Medicine, Kyoto University Faculty of Medicine, 54 Kawahara-cho, Shogoin, Sakyo-ku, Kyoto, 606 Japan.

TABLE 1
Patients Characteristics and Radionuclide Imaging Results

Patient no.	Age/Sex	Site of tumor	Size (mm)	Histological type	PET (T/N R)	SPECT (T/N R)
1	68/M	Body	55	adenoca.	+(3.49)	+(1.77)
2	72/M	Tail	60	moderately diff. tubular adenoca.	+(2.18)	+(1.72)
3	68/F	Uncus	50	moderately diff. tubular adenoca.	+(3.17)	+(1.30)
4	76/F	Head	70	moderately diff. tubular adenoca.	+(2.33)	+(1.50)
5	66/M	Head	70	poorly diff. tubular adenoca.	+(5.84)	+(1.30)
6	44/F	Head	37	poorly diff. tubular adenoca.	+(1.65)	+(2.00)
7	58/M	Body	50	adenoca.	+(3.61)	+(1.80)
8	55/F	Body	55	moderately diff. tubular adenoca.	+(3.45)	+(2.52)
9	42/M	Head	80	adenoca.	+(2.49)	+(1.61)
10	60/F	Uncus	40	adenoca.	+(3.99)	+(1.49)
11	69/M	Body	80	moderately diff. tubular adenoca.	+(5.84)	+(1.65)
12	46/M	Head	70	adenoca.	+(4.02)	+(2.44)
13	59/F	Head	50	poorly diff. tubular adenoca.	+(4.00)	+(2.01)
14	64/F	Body	40	poorly diff. tubular adenoca.	+(2.72)	+(2.19)
15	57/M	Head	20	moderately diff. tubular adenoca.	+(3.65)	+(1.42)
16	67/F	Head	80	adenoca.	+(3.77)	+(1.65)
17	37/M	Body	50	adenoca.	+(4.51)	—
18	45/M	Uncus	70	mucinous cystadenoca.	+(2.09)	—
19	42/M	Head	35	moderately diff. tubular adenoca.	+(1.85)	—
20	54/M	Body	100	moderately diff. tubular adenoca.	+(2.74)	—
21	77/M	Head	30	mucinous cystadenoca.	+(1.87)	—
22	72/M	Tail	80	adenoca.	+(5.14)	—
23	67/F	Head	20	mucinous cystadenoca.	+(1.62)	—
24	69/F	Ampulla	15	well diff. tubular adenoca.	+(1.67)	—
25	62/M	Body	10	mucinous cystadenoca.	—	—

cut-off frequency of 0.5 cycle/pixel. No attenuation correction was performed.

FDG-PET

On the same day, PET was performed using a whole-body PET camera (PCT 3600W, Hitachi Medico Co., Tokyo, Japan), which has 8 rings; providing 15 tomographic slices at 7-mm intervals. The intrinsic resolution was 4.6 mm FWHM at the center, and the axial resolution was 7 mm FWHM. The effective resolution after reconstruction was approximately 10 mm. Each subject was positioned on the PET camera using the ultrasound technique and underwent transmission scanning for attenuation correction for 20 min. Immediately after the transmission scan, approximately 150 MBq (4 mCi) of FDG were administered intravenously, and static scan was performed 60 min later for 15 min.

Data Analysis

For qualitative analysis, any obvious foci of increased FDG or ^{201}Tl uptake over background not located in areas of physiological tracer uptake and/or excretion to the gastro-intestinal tract were considered positive for tumor. The degree of FDG and ^{201}Tl activities in the tumor were visually scored using a four-point grading system: no uptake (grade 0), equivocal (grade 1), mildly increased (grade 2) and definitely increased uptake (grade 3). Uptake rated as grade 2 or 3 was considered to represent significant tracer accumulation.

For quantitative analysis of the FDG uptake, the standardized uptake value (SUV = tumor activity concentration/injected dose/body weight) was calculated. Following 10 × 10 mm square ROIs were selected in areas of the tumor showing the highest FDG activity and in the normal pancreas; the SUVs were calculated

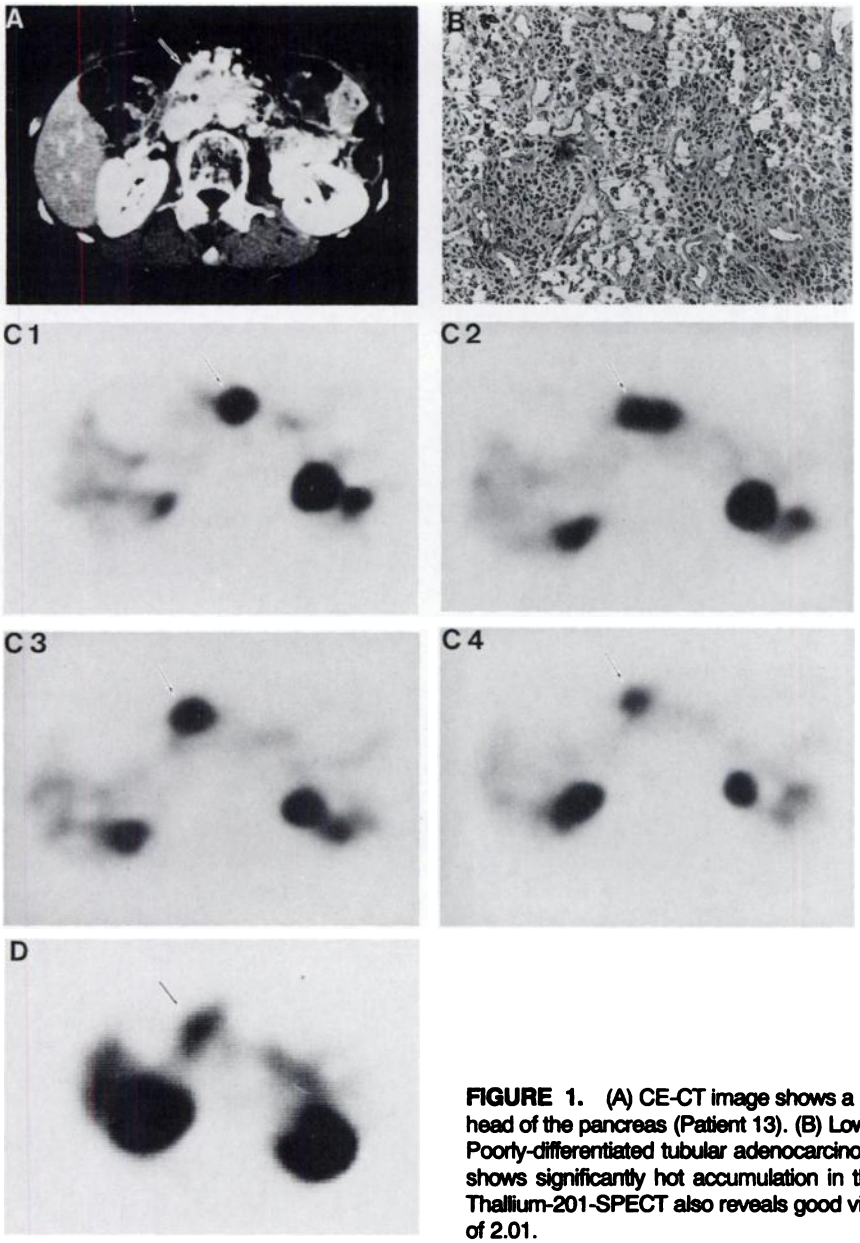

FIGURE 1. (A) CE-CT image shows a heterogeneously-enhanced mass (arrow) in the head of the pancreas (Patient 13). (B) Low magnification of the tumor (H&E stain, 100×). Poorly-differentiated tubular adenocarcinoma is seen. (C) FDG-PET (four serial images) shows significantly hot accumulation in the tumor (arrow) with a T/N ratio of 4.00. (D) Thallium-201-SPECT also reveals good visualization in the tumor (arrow) with a T/N ratio of 2.01.

using a calibration factor between PET counts and radioactivity concentration. In addition, tumor to nontumor activity ratio of the SUV (T/N ratio) was calculated. On the other hand, for semiquantitative analysis of ^{201}Tl-SPECT, the radioactivity was measured for areas of the tumor showing the highest ^{201}Tl accumulation and in the normal pancreas by taking a 10 × 10 mm^2 ROI to calculate the tumor to nontumor ratio of the activity (T/N ratio).

Statistical Analysis

Comparison of differences in the T/N ratio of FDG and ^{201}Tl uptakes was performed using the two-tailed Student's t-test for unpaired data. Probability values of less than 0.05 were considered to be statistically significant.

RESULTS

Table 1 summarizes the results of the radionuclide and pathological findings for the 25 patients studied.

Visual Analysis

FDG-PET showed an increase in tracer uptake in the tumor in 24 of 25 patients (96%) (Table 1). An FDG-negative case (Patient 25) of one mucinous cystadenocarcinoma papillary grown into the main pancreatic duct of 10 mm in diameter was not visualized by CT, US or MRI images except in endoscopic ultrasonography.

On the other hand, ^{201}Tl-SPECT showed an increase in tracer uptake in 16 patients (64%). In those patients, increased tracer accumulation was also observed by FDG-PET (Fig. 1). Among the nine remaining patients with no significant ^{201}Tl uptake on SPECT, spotty accumulation of FDG was detected in a solid component (15–25 mm in size) of three mucinous cystadenocarcinomas (Patients 18, 21 and 23, Fig. 2), and definite FDG accumulation was ob-

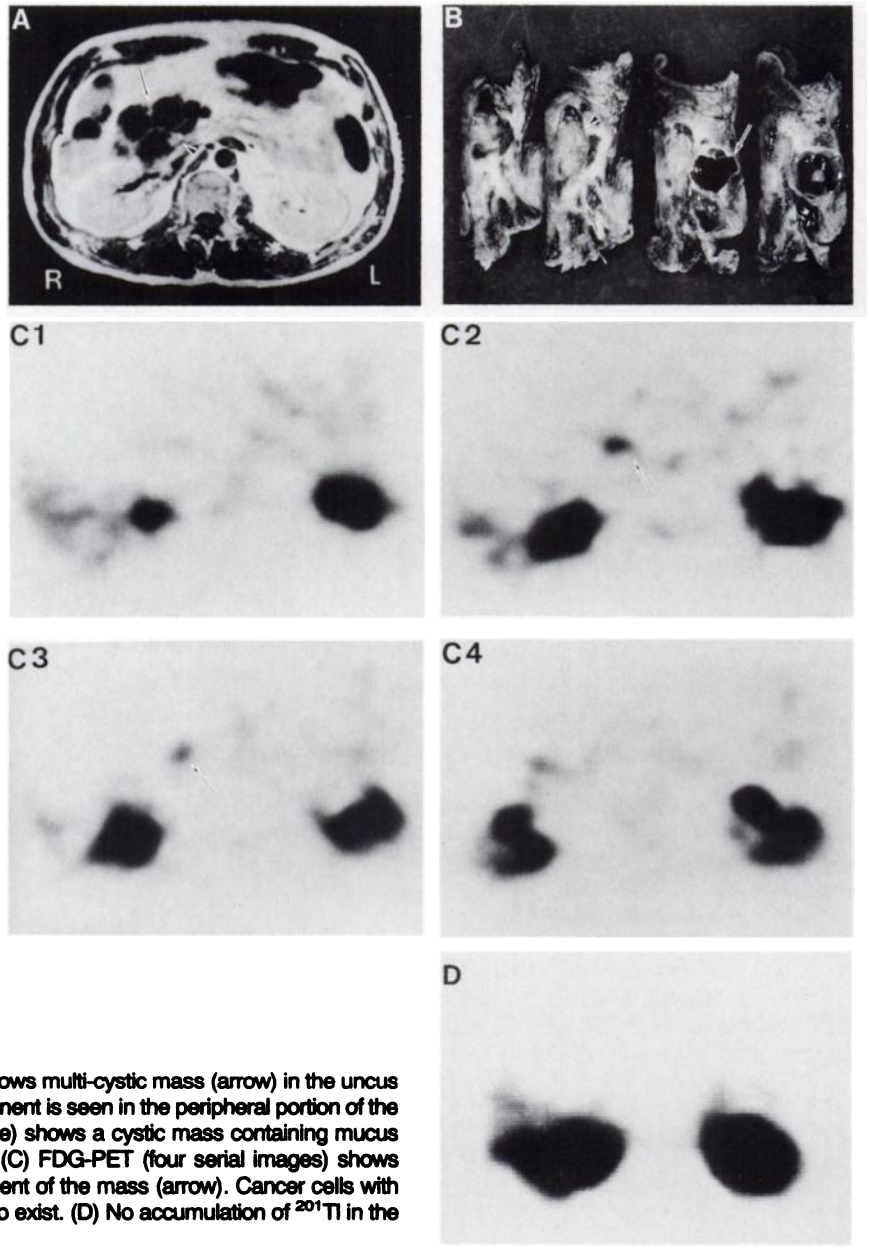

FIGURE 2. (A) MRI (T1 weighted image) shows multi-cystic mass (arrow) in the uncus of the pancreas (Patient 18). Small solid component is seen in the peripheral portion of the mass (arrow). (B) Resected specimen (cut slice) shows a cystic mass containing mucus (arrow) and a solid component (arrow head). (C) FDG-PET (four serial images) shows spotty tracer accumulation in the solid component of the mass (arrow). Cancer cells with accelerated glucose metabolism were proven to exist. (D) No accumulation of ^{201}Tl in the tumor site.

served in four adenocarcinomas (Patients 17, 19, 20 and 22, Fig. 3). In case of ampullary carcinoma (15 mm in size) located in the end of the common bile duct, obstructive jaundice was the first clinical manifestation. At first evaluation, pin-point uptake of FDG was not considered positive for tumor. Although comparison with the corresponding CT images proved that FDG accumulation clearly indicated the tumor site with the T/N ratio of 1.67 (Patient 24).

The mean visual score of ^{201}Tl-SPECT (2.31 ± 0.48) was significantly lower than that of FDG-PET (2.79 ± 0.38) in the positive cases ($p < 0.005$).

Quantitative Analysis

The T/N ratio of FDG ranged from 1.62 to 5.84 with a mean of 3.24 ± 1.27 (n = 24) in the FDG-positive cases (Fig. 4). Meanwhile, the T/N ratio of ^{201}Tl ranged from 1.30 to 2.52, with a mean of 1.71 ± 0.37 (n = 16), which was significantly less than that of FDG ($p < 0.0001$) (Table 1).

DISCUSSION

The present study demonstrated that pancreatic cancer can be visualized as an increase in tracer accumulation by both ^{201}Tl-SPECT and FDG-PET. However, FDG-PET provided better sensitivity for detecting pancreatic cancer and a higher T/N ratio than ^{201}Tl-SPECT.

Noninvasive diagnosis of pancreatic cancer is of clinical importance for early and curative treatment. However, it is sometimes difficult to differentiate pancreatic tumors malignant or benign. A number of PET and SPECT studies have been attempted to identify pancreatic lesions using

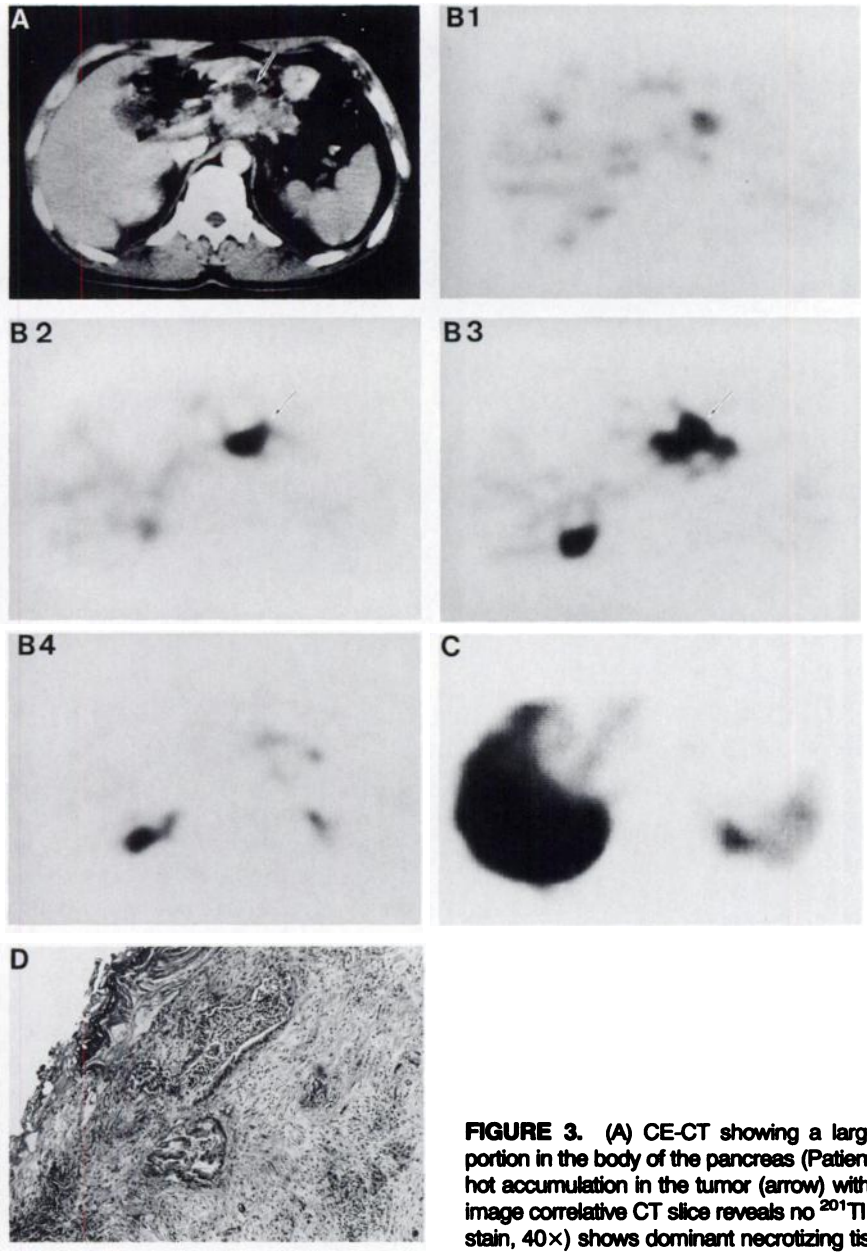

FIGURE 3. (A) CE-CT showing a large mass (arrow) with poor-enhanced necrotic portion in the body of the pancreas (Patient 20). (B) FDG-PET (four serial images) shows hot accumulation in the tumor (arrow) with a T/N ratio of 2.74. (C) Thallium-201-SPECT image correlative CT slice reveals no ^{201}Tl accumulation. (D) Histological specimen (H&E stain, 40×) shows dominant necrotizing tissue with scarce cancer cells.

^{11}C-methionine or ^{123}I-HIPDM (*27,28*). Since these tracers accumulated in the normal pancreatic tissue and focal lesions were seen as cold spots, it is difficult to differentiate focal tumor lesions from generalized decreased function of the pancreas, such as chronic pancreatitis in the case of decreased tracer accumulation in the pancreas. FDG and ^{201}Tl have the potential to identify malignant tumors as areas of tracer accumulation.

Value of FDG-PET

FDG has found widespread use in PET and is considered to be a standard radiopharmaceutical for metabolic studies. Its role as a tumor-seeking agent has been established in many different types of malignant tumors (*8–15*). FDG accumulation in tumors is induced by activation of glucose transporters and elevated glucose consumption, which are considered to be early and prominent features of oncogene-mediated malignant transformation in cell culture systems (*31*).

A recent report demonstrated an increase in glucose transporter one gene expression in human pancreatic cancer cells (*32*), and FDG is clearly accumulated in pancreatic cancer (*16*). Because of its low rate of dephosphorylation, FDG is transported, phosphorylated and metabolically trapped in tumor cells as fluorodeoxyglucose-6-phosphate. Therefore, pancreatic cancer can be visualized clearly with FDG.

In this study, 24 of 25 pancreatic cancers were detected as an increase in FDG accumulation. The tumors of only one patient (Patient 25) were not visualized in the PET study. In such a case, the tumor was too small in size (10 mm in diameter) to be detected by the current PET system,

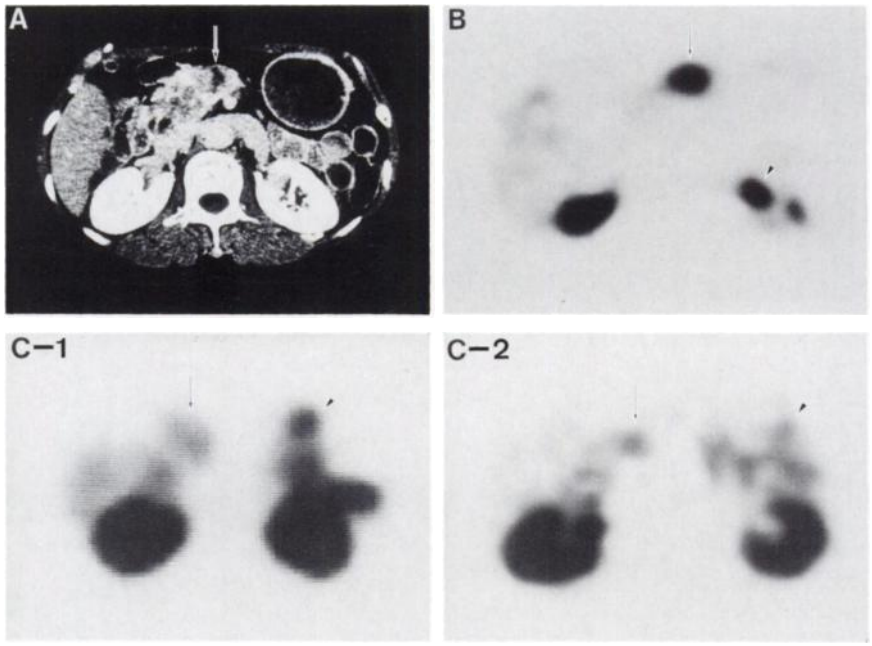

FIGURE 4. (A) CE-CT shows irregular-margined low density mass (arrow) in the body of the pancreas (Patient 8). (B) FDG-PET shows significantly hot accumulation in the tumor (arrow) with a T/N ratio of 3.45. FDG accumulation in the left ureter is also observed centrally (arrow head). (C) Comparison of ^{201}Tl-SPECT images using a single-head camera system (C-1) and a three-head camera system (C-2). The image quality is superior in the latter, however, the T/N ratio of the activity has not improved. Significantly high tracer accumulation in the stomach and intestine is observed on both SPECT images (arrow head).

which has poor spatial resolution compared with x-ray CT imaging. However, the sensitivity value of 96% seems to be satisfactory.

Value of Thallium-201-SPECT

Thallium-201 uptake is considered to reflect the regional perfusion and viability of tumor cells (*17,18,26*). This technique has been shown to be useful for detecting malignant tumors in the lung and thyroid (*17–20*). Regarding the mechanism of ^{201}Tl accumulation in tumors, a relationship to Na-KATPase has been reported (*23*). In a study of pancreatic cancer, Togawa et al. (*24*) reported preliminary results showing the value of ^{201}Tl-SPECT in the delineation of the tumor as a hot spot. Our results are in accord with their preliminary data. Because of the low expense and ready availability of SPECT cameras in most clinical centers, ^{201}Tl-SPECT may offer alternative means for evaluation of suspected pancreatic cancer. Another advantage of ^{201}Tl-SPECT is to provide coronal and sagittal slices. These images are helpful to identify pancreatic head and tail lesions separately from adjacent organs.

Comparison of These Techniques

Although ^{201}Tl-SPECT detected pancreatic cancer in the majority of these patients, the sensitivity of ^{201}Tl-SPECT was inferior to that of FDG-PET, with a lower visual score for ^{201}Tl-SPECT than for FDG-PET in the positive cases. Furthermore, quantitative data also indicated a lower T/N ratio on ^{201}Tl-SPECT than that on FDG-PET. In the FDG-negative case, ^{201}Tl-SPECT also did not show significant accumulation. On the other hand, in eight FDG-positive cases of 15–100 mm in diameter, ^{201}Tl uptake was not seen. Histological studies suggested the presence of necrotic tissue around the tumor cells in most of these cases, as shown in Figure 3, except for several tiny tumors. This is in agreement with the preliminary report of Togawa et al. (*24*) showing that predominantly necrotized tumors with scarce viable tissue reveal no accumulation of ^{201}Tl. CE-CT showed poor enhancement in these cases. In such cases, FDG-PET should play an important role in delineating viable tumors.

Several reasons for the discordance between FDG and ^{201}Tl distributions are possible. First, the mechanisms of the accumulation of these tracers in tumors are completely different, as described previously. As a marker of exogenous glucose utilization, FDG accumulates in high-grade malignant tumors (*29*) and therefore seems to be a more specific marker to characterize tumor malignancy. Second, differences in the background activity may strikingly alter the T/N ratio. While mild accumulation of FDG was observed in the surrounding tissue, ^{201}Tl background-accumulation in tissues such as the stomach and intestine was quite high. To minimize such background activity, each patient was fasted overnight prior to the tests. However, high accumulation was still observed in these tissues, which could obscure the tumor activity on ^{201}Tl-SPECT images. Less FDG activity in the stomach and intestine caused a much higher T/N ratio. Third, the spatial resolutions between PET and SPECT were strikingly different. The effective resolution after reconstruction was about 10 mm with PET and 17 mm with SPECT. The lower resolution with ^{201}Tl-SPECT may cause a greater partial volume effect, and thus lower the target to nontarget count ratio. Fourth, the sensitivities of the cameras were also strikingly different. PET showed about 10 times greater counts per slice than SPECT within similar acquisition times, which may cause a great difference in image quality. In the current study, we used a single-head rotating gamma camera, though it was suggested that a newer multi-head SPECT camera may improve the image quality of ^{201}Tl-SPECT. In the latter seven cases, ^{201}Tl-SPECT was performed continuously with three-head SPECT camera (PRISM 3000,

Shimazu Co., Kyoto, Japan). Although, the image quality of ^{201}Tl-SPECT was improved to a certain degree, sensitivity and T/N ratio of tracer uptake did not change (Fig. 4).

Limitations

This study has a number of limitations. First, ^{201}Tl-SPECT was performed only during the first 15 min after tracer administration for comparison with FDG-PET. The value of delayed ^{201}Tl scan 3 hr after tracer administration has been reported for differentiating malignant from benign tumors (*19,30*). However, a higher background of ^{201}Tl in the surrounding tissue may obscure the tumor activity on the delayed scan. In addition, each patient would have to wait an additional 3 hr (a total of 5 hr) for the whole PET and SPECT studies, which may be rather impractical for clinical investigations.

Second, this study included only cases of histologically-proven pancreatic cancer. Therefore, while the true-positive rate for these studies can be calculated, the true-negative rate could not be evaluated. In this respect, a prospective analysis of patients with suspected pancreatic cancer may be warranted for comparing the diagnostic accuracy of these techniques.

Third, in blinded evaluation without CT and/or MRI imaging, signal-to-noise ratio of ^{201}Tl-SPECT is too low to distinguish the tracer uptake of the tumor from significantly high tracer excretion and accumulation to the stomach and intestine. This is quite a limitation of ^{201}Tl for the intra-abdominal tumor seeking agent. In our study, correct image correlation between CT and SPECT images was necessary for detailed evaluation. On the other hand, FDG accumulation of the tumor was high enough to evaluate the images without other imaging results.

CONCLUSIONS

In this comparative study, both techniques (FDG-PET and ^{201}Tl-SPECT) delineated tumors as sites of high tracer accumulation. Yet, FDG-PET provided significantly higher sensitivity and higher contrast than ^{201}Tl-SPECT. Therefore, both FDG-PET and ^{201}Tl-SPECT should be considered to have clinical value for the noninvasive detection of pancreatic cancer. However, if a PET camera is available, FDG-PET is considered to be the method of choice for the evaluation of patients with suspected pancreatic cancer.

REFERENCES

1. Silverberg E, Lubera J. Cancer statistics, 1986. *Cancer J Clin* 1986;36:9–25.
2. Som P, Atkins AD, Bandoypadhyay D, et al. A fluorinated glucose analogue, 2-fluoro-2-deoxy-D-glucose (F-18): nontoxic tracer rapid tumor detection. *J Nucl Med* 1980;21:670–675.
3. Larson SM, Weiden PL, Grunbaum Z, et al. Positron imaging feasibility studies. II. Characteristics of 2-deoxyglucose uptake in rodent and canine neoplasms. Concise communication. *J Nucl Med* 1981;22:875–879.
4. Abe Y, Matsuzawa T, Fujiwara T, et al. Assessment of radiotherapeutic effects on experimental tumors using F-18-2-fluoro-2-deoxy-D-glucose. *Eur J Nucl Med* 1986;12:325–328.
5. Kubota K, Ishiwata K, Kubota R, et al. Tracer feasibility for monitoring tumor radiotherapy: a quarruple tracer study with fluorine-18-fluorodeoxyglucose or fluorine-18-fluorinedeoxyuridine, L-(methyl-^{14}C)methionine, (6-^{3}H) thymidine and gallium-67. *J Nucl Med* 1991;32:2118–2123.
6. Wahl RL, Hutchins GD, Buchsbaum D, Liebert M, Grossman HB, Fisher S. ^{18}F-2-deoxy-2-fluoro-D-glucose uptake in human tumor xenografts. *Cancer* 1991;67:1544–1550.
7. Haberkorn U, Reinhardt M, Strauss LG, et al. Metabolic design of combination therapy: use of enhanced fluorodeoxyglucose uptake caused by chemotherapy. *J Nucl Med* 1992;33:1981–1987.
8. Yonekura Y, Benua RS, Brill AB, et al. Increased accumulation of 2-deoxy-2-(^{18}F) fluoro-D-glucose in liver metastases from colon cancer. *J Nucl Med* 1982;23:1133–1137.
9. Minn H, Paul R, Ahonen A. Evaluation of treatment response to radiotherapy in head and neck cancer with fluorine-18-fluorodeoxyglucose. *J Nucl Med* 1988;29:1521–1525.
10. Kubota K, Matsuzawa T, Fujiwara T, et al. Differential diagnosis of lung tumor with positron emission tomography: a prospective study. *J Nucl Med* 1990;31:1927–1933.
11. Wahl RL, Cody RL, Hutchins CD, Mudgett EE. Primary and metastatic breast carcinoma: initial clinical evaluation with PET with the radiolabeled glucose analogue 2-(F-18)-fluoro-2-deoxy-D-glucose. *Radiology* 1991;179:765–770.
12. Ichiya Y, Kuwabara Y, Otsuka M, et al. Assessment of response to cancer therapy using fluorine-18-fluorodeoxyglucose and positron emission tomography. *J Nucl Med* 1991;32:1655–1660.
13. Strauss LG, Conti PS. The application of PET in clinical oncology. *J Nucl Med* 1991;32:623–648.
14. Hawkins RA, Hoh C, Dahlbom M, et al. PET cancer evaluations with FDG. *J Nucl Med* 1991;32:1555–1558.
15. Ito K, Kato T, Tadokoro M, et al. Recurrent rectal cancer and scar: differentiation with PET and MR imaging. *Radiology* 1992;182:549–552.
16. Klever P, Bares R, Fass J, et al. PET with fluorine-18 deoxyglucose for pancreatic disease. *Lancet* 1992;340:1158–1159.
17. Togawa T, Suzuki A, Kato K, et al. Relation between Tl-201 to Ga-67 uptake ratio and histological type in primary lung cancer. *Eur J Cancer Clin Oncol* 1985;21:1263.
18. Senga O, Miyakawa M, Shirota H, et al. Comparison of Tl-201 chloride and Ga-67 citrate scintigraphy in the diagnosis of thyroid tumor: concise communication. *J Nucl Med* 1982;23:225–228.
19. Tonami N, Shuke N, Yokoyama K, et al. Thallium-201 single photon emission computed tomography in the evaluation of suspected lung cancer. *J Nucl Med* 1989;30:997–1004.
20. Matsuno S, Tanabe M, Kawasaki Y, et al. Effectiveness of planar image and single emission tomography of Tl-201 compared with Ga-67 in patients with primary lung cancer. *Eur J Nucl Med* 1992;19:86–95.
21. Ando A, Ando I, Katayama M, et al. Biodistributions of Tl-201 in tumor bearing animals and inflammatory lesion induced animals. *Eur J Nuc Med* 1987;12:567–572.
22. Ito Y, Muranaka A, Harada T, et al. Experimental study on tumor affinity of ^{201}Tl-chloride. *Eur J Nucl Med* 1978;3:81–86.
23. Elligsen JD, Thompson JE, Frey HE, et al. Correlation of Na-KATPase activity with growth of normal and transformed cells. *Exp Cell Res* 1974; 87:233–240.
24. Togawa T, Yui N, Kinoshita F, et al. Diagnosis of pancreatic cancer using Tl-201 chloride and a three-head rotating gamma camera SPECT system. *Kaku Igaku* 1991;28:1475–1481.
25. Yonekura Y, Tamaki N, Kambara H, et al. Detection of metabolic alteration in ischemic myocardium by F-18 fluorodeoxyglucose uptake with positron emission tomography. *Am J Cardiac Imaging* 1988;2:122–132.
26. Tamaki N, Yonekura Y, Yamashita K, et al. Relation of left ventricular perfusion and wall motion with metabolic activity in persistent defects on thallium-201 tomography in healed myocardium infarction. *Am J Cardiol* 1988;62:202–208.
27. Buonocore E, Hubner KF. Positron emission computed tomography for the pancreas: a preliminary study. *Radiology* 1979;133:195–201.
28. Yamamoto K, Shibata T, Saji H, et al. Human pancreas scintigraphy using iodine-123-labeled HIPDM and SPECT. *J Nucl Med* 1990;31:1015–1019.
29. DiChiro G, et al. Glucose utilization of cerebral gliomas measurement by F-18 fluorodeoxyglucose and positron emission tomography. *Neurology* 1982;22:360–371.
30. Ochi H, Sawa H, Fukuda T, et al. Thallium-201 chloride thyroid scintigraphy to evaluate benign and/or malignant nodules: usefulness of the delayed scan. *Cancer* 1982;50:236–240.
31. Flier JS, Mueckler MM, Usher P, et al. Elevated levels of glucose transport and transporter messenger RNA are induced ras or src oncogenes. *Science* 1987;235:1492–1495.
32. Kornrumpf P, Buchler M, Langhans J, et al. Concordantly increased glucose transporter 1 (GLUT 1) gene expression and FDG uptake in human pancreatic carcinoma [Abstract]. *J Nucl Med* 1993;34:223.